

# Design and Development of a Software-Defined Underwater Acoustic Modem for Sensor Networks for Environmental and Ecological Research

Tricia Fu, Daniel Doonan, Chris Utley, Ronald Iltis, Ryan Kastner, and Hua Lee  
Department of Electrical and Computer Engineering  
University of California  
Santa Barbara, CA 93106 USA

**Abstract**-This paper describes the design and successful development of an acoustic modem for potential use in underwater ecological sensor networks. The presentation includes theoretical study, design and development of both software and hardware, laboratory experiments, and the documentation and analysis of field-test results.

## I. INTRODUCTION

Advances in communication and sensor technology will continue to enhance our capability of monitoring the natural world, which is critical in environmental science. Advanced sensing systems provide us with the ability to perform a wide range of real-time, large-scale experiments to monitor complex ecosystem processes. Fundamental to these efforts is a broad suite of environmental observations ranging from basic environmental parameters such as water temperature, salinity and bio-optical variables, to more complex measurements such as nutrient concentration, the level of environmental estrogens, volatile hydrocarbons, and pathogenic bacteria. More complex observations include monitoring the migration of fishes and other aquatic animals across large ocean areas with various tagging approaches.

The overall objective of the new AquaNode initiative is the design and development of an enabling communication network to facilitate multi-unit underwater sensing experiments. The system will be capable of conducting underwater sensing and imaging experiments through three communication layers: (1) the interface stations over the ocean surface, (2) underwater base stations, and (3) the sensing and imaging units, all capable of operating in mobile mode.

One of the most challenging elements is the design and development of a software-defined acoustic modem for the communication among the underwater sensor units at all three layers. Furthermore, as the survey modality advances forward toward mobile autonomous sensing, the acoustic modem will also be responsible for (a) navigation and guidance, (b) sensor data harvesting, and (c) remote interactive sensing and imaging experiments.

The acoustic modem has previously been designed at the algorithmic level, and employs Walsh/m-sequence signaling with Matching Pursuits (MP) channel estimation [1]. Here, a software-defined implementation of the modem in the TI C6713 DSP device is presented. An optimized version of the MP channel estimation algorithm [2], [1] is developed for real-time operations. The modem will operate with a bandwidth of 6 kHz at a center frequency 24 kHz, with a data rate of 161 bps. The performance of channel order estimation based on MP residuals is verified.

This research project represents a direct and optimal integration of communication signal processing techniques, hardware-software integration, and network protocols. Because of the area spread of the experiment sites, the modem design has also incorporated the technical elements of communication range, multi-path interference removal and reduction, simplicity for effective manufacture and maintenance, and power assumption level. Although the focus of this program is on the environmental and ecological research, the successful execution of this project will make profound impacts on various commercial applications.

## II. HARDWARE IMPLEMENTATION

The prototype hardware is a mixture of commercial off-the-shelf systems (e.g. DSP evaluation board), systems assembled from standard components (e.g. amplifiers) and components custom-made to spec (e.g. transducers). Fig. 1 shows the prototype hardware setup for a tank test. In a 'production' version, the electronic components would be integrated onto custom circuit boards to remove functions which would no longer be necessary (e.g. real-time debugging).



Figure 1. Left: DSP Boards, transmitter amplifier and battery. Right: Top view of Sonatech transducer partially submerged in saltwater tank.

System power is supplied in the field by batteries. For testing purposes lead-acid secondary cells (Pb/PbO<sub>2</sub>) are used. Since recharging is assumed to be unavailable in the field, however, alkaline primary cells (Zn/MnO<sub>2</sub>) are more cost-effective for most deployments. More exotic chemistries may be used if required; for example, Li/MnO<sub>2</sub> and Li/SOCl<sub>2</sub> have far higher energy densities.

Very little signal processing is conducted in hardware. The analog↔digital conversions are performed with passband signals, so modulation and demodulation are entirely digital. Only amplification and antialiasing/reconstruction filters are implemented in hardware. This minimizes hardware cost and complexity while maximizing flexibility.

### III. SOFTWARE IMPLEMENTATION

The Matching Pursuits (MP) algorithm [3] provides an estimator for sparse channels [2, 4] – the basis for both symbol decision (MPDetect) and symbol synchronization (MPSync) algorithms [1]. Software implementations for both MPDetect and MPSync, in addition to the signaling scheme, were detailed in [5].

#### A. Increased Number of Training Symbols

Since each synchronization error causes a number of symbol errors, ways to improve MPSync are currently being investigated. One recent testing change was to increase the number of training symbols passed to MPSync from 2 to 5. Fig. 2 illustrates how in the estimated multipath intensity profile (MIP), the increased number of training symbols improved channel estimates so that there were less whole packet misalignments. In the MIP, the horizontal axis indicates the delay, in ms, for a path, line intensity indicates path strength, and the vertical axis indicates for which transmitted symbol in the entire message, e.g. the tenth, the channel estimate applies to.

#### B. Channel order ( $N_f$ ) estimation

An additional improvement to our MP-based modem was to estimate channel order ( $N_f$ ) using the timing acquisition algorithm MPSync [1]. Table 1 shows the relevant equations for channel order estimation according to the MP-algorithm described in [1].

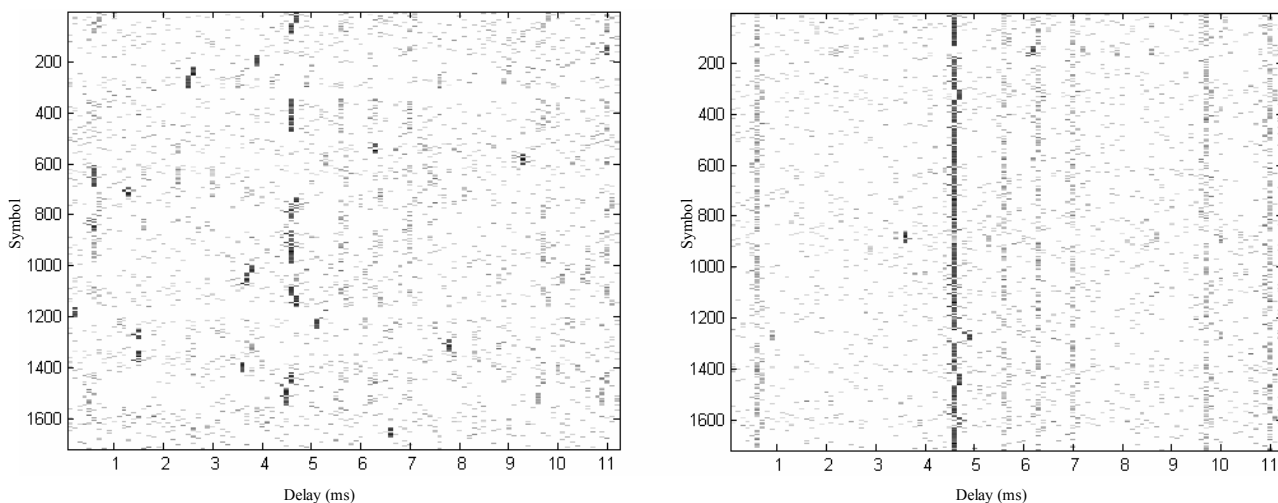


Figure 2. Estimated Multipath Intensity Profile (MIP) from simulations, actual number of multipaths = 10, SNR = -4 dB. Left: 2 training symbols, and estimated  $N_f$  varying from 1 to 16 with SER = 0.6645. Right: 5 training symbols, and estimated  $N_f$  varying from 5 to 16 with SER = 0.1023.

TABLE 1  
MPSYNC CHANNEL ORDER ESTIMATION ALGORITHM

```

 $r = Sf + n$ 
 $v^1 = S^H r \in C^{2N_s}$ 
 $\epsilon = 0.01v^1$ 
...
For  $k = 1, 2, \dots, N_{\max}$ 
    ...
     $v^{k+1} = v^k - A(:, q_k) \hat{f}_{q_k}$ 
    If  $\|v^k\|^2 - \|v^{k+1}\|^2 < \epsilon$ 
        Estimated channel order is  $k$ 
        Break
    End If
Next  $k$ 

```

In Table 1,  $r$  refers to the received sample vector. The initial value of the sufficient statistic vector,  $v^1$ , is the correlation between the received vector and the expected training symbol. The update equation for  $v^k$  shows how the strongest signal components are iteratively cancelled. The variable  $\epsilon$  is set to a percentage of the correlation  $v^1$ , and  $N_{\max}$  is set to the largest number of multipaths expected in the channel.

The channel order estimation is based on the norm of the  $v^k$ . After a cancellation, if the difference between successive  $v^k$  norms falls below threshold  $\epsilon$ , MPSync stops the cancellation process. It then returns the number of cancellations as the number of hypothesized multipaths, i.e. the estimated channel order.

#### IV. WIRE TEST RESULTS

Wire tests were conducted for intermediate debugging purposes using audio cables between two C6713 DSP boards. The ADC/DAC sampling rate was set to 96 kHz. To provide SNR estimates for this test and tests in other environments, arrays of unprocessed data from the ADC with the transmitter on and with the transmitter off were saved. Each element of the arrays was squared, then summed and divided by the number of elements to provide energy measurements. The ratio of energy with transmitter on to the energy with transmitter off minus one yielded the linear SNR measure, from which the power SNR measure (in dB) was calculated.

The high SNR environment (57.4 dB) yielded 0 symbol error rates during various trials. Each trial duration for the wire test was 100 packets with 43 symbols per packet, with MPSync taking 5 training symbols rather than the minimum of 2. Average Doppler spread was 0.0623 Hz, and the channel

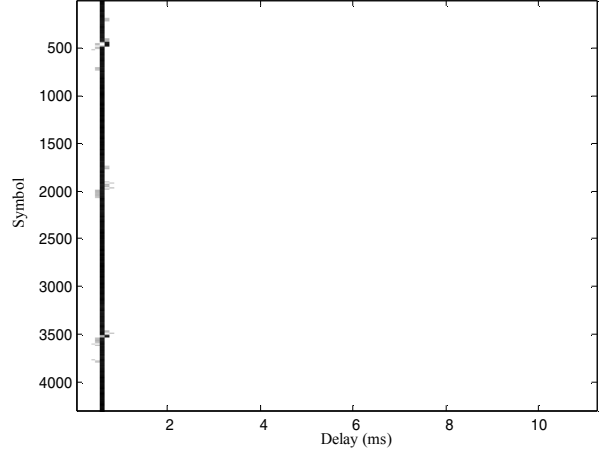


Figure 3. Multipath Intensity Profile (MIP) in wire test, and  $N_f$  varying from 1 to 2.

order estimation software registered 1 to 2 paths, when the actual transmitted signal had only 1 path. Fig. 3 shows a sample multipath intensity profile (MIP) for the wire tests.

#### V. AIR TEST RESULTS

##### A. In-lab Air Test

From the MIP in Fig. 4, the well-delineated paths indicated that this was another high SNR environment; later measurements gave an SNR of 11.8 dB. Standard computer speakers and a microphone were used as transducer substitutes, with a 6 ft distance between the two. With ADC/DAC sampling rate set to 8 kHz, the average Doppler spread was 0.1038 Hz, and in all trials the symbol error rate was zero with the test duration at 6 packets. The channel order estimates ranged from 2 to 8 for various trials.

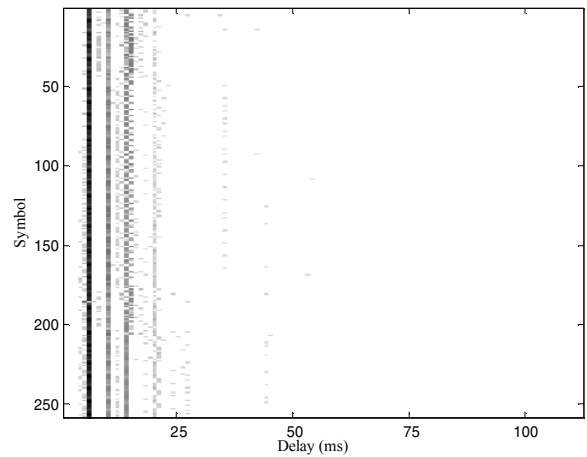


Figure 4. Sample MIP for in-lab air test,  $F_s = 8$  kHz,  $N_f$  varying from 5 to 6, 11.8 dB SNR, 6 ft distance

TABLE 2  
HALLWAY AIR TEST RESULTS

Trial	SER	Doppler Spread (Hz)
1	0.0233	0.173
2	0	0.1903
3	0	0.1557

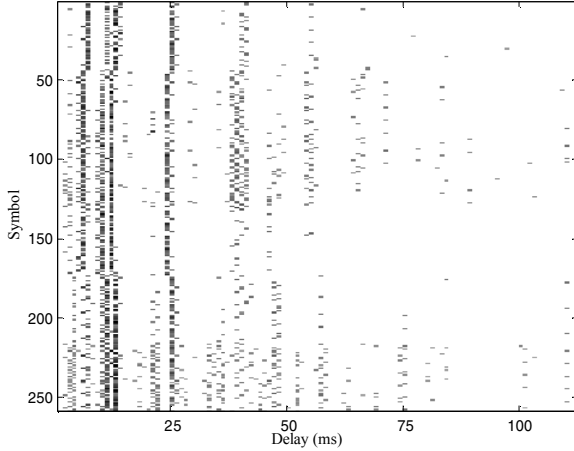


Figure 5. Sample MIP for hallway air test,  $F_s = 8$  kHz,  $N_f$  varying from 3 to 12

### B. Hallway Air Test

The receiver microphone and transmitter speaker were placed 117 ft apart in the UCSB Harold Frank Hall third floor hallway, with the receiver and transmitter sampling rate set to 8 kHz. Each test duration was 6 packets, with 43 symbols per packet. The test results for three trials, shown in Table 2, were characterized by low symbol error rate and Doppler spreads of less than 0.2 Hz for each test. Only 2 training symbols at a time were used for timing acquisition.

The  $N_f$  estimation software in each case hypothesized a wide range of number of multipaths, ranging from 3 to 14 between packets. Fig. 5 shows a sample MIP for the hallway air test's third trial.

### C. Stairway Air Test

The most challenging in-air test was the stairway test, held in the UCSB Harold Frank Hall east stairway. In a preliminary trial in the stairway the modem would not yield an SER of less than 0.5. The resulting channel estimate plots indicated that Inter-Symbol Interference (ISI) was the main source of the problem. Thus, a software version supporting a variable-length guard time was developed. In all other tests, wire or air or water, the guard time had been set to the same as the transmit duration.

TABLE 3  
STAIRWAY AIR TEST RESULTS

Trial	NF	Guard Time	SER	Doppler Spread (Hz)
1	20	9	0.0078	0.0069
2	20	11	0	0.0029
3	30	11	0.0078	0.0029

For each test, Table 3 lists the guard time as a multiple of the transmit duration, the symbol error rate, and the Doppler spread. At the time of the test, no  $N_f$  estimation had been implemented, so  $N_f$  had been fixed to a high value. The test setup placed the receiver on the third floor, with the transmitter on the fourth floor. The stairwell connected the first through fifth floors. Test duration was again 6 packets, 43 symbols per packet, with sampling rate set to 8 kHz.

The indicated Doppler spread is quite low, but this is in large part due to the much lower symbol rate resulting from the longer guard time. The MIP for Trial 2 is shown in Fig. 6, with the horizontal axis reduced from 1200 ms to 500 ms due to lack of paths in the delay range greater than 500 ms.

## VI. TANK TEST RESULTS

Water tests were conducted at UCSB's Marine Biotechnology Laboratory, seawater processing room, using the DSP board's maximum sampling rate of 96 kHz to support the 24 kHz center frequency used with the transducers. The available tank was a relatively noisy environment due to nearby pumps and machinery. In the first series of tests (A), the transducers were separated by various distances, 0.6 and 12.7 meters, and no  $N_f$  estimation was performed. Also, only 2 training symbols were used for timing acquisition. Tank access through hatches precluded the use of intermediate distances. A later series of tests (B) was performed with the integrated  $N_f$  estimation software and increased number of training symbols passed to MP Sync, however problems with the transmitter's amplifier severely impaired performance.

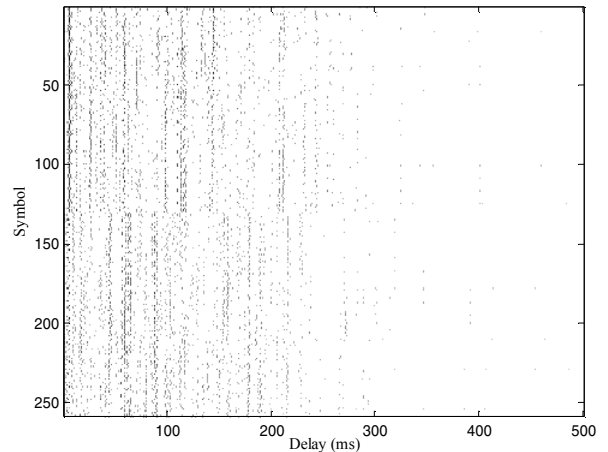


Figure 6. Sample MIP for stairway air test,  $F_s = 8$  kHz, and  $N_f = 20$ .

TABLE 4  
TANK TEST RESULTS, SERIES A, FIXED  $N_f$  AND 2 TRAINING SYMBOLS

Distance	NF	SER	Doppler Spread (Hz)
0.60 m	6	0	0.218
	3	0.025	0.1246
	2	0	0.1869
	1	0	0.218
12.7 m	13	0.2959	0.9967
	10	0.1192	0.9344

### A. Short distance (0.60 m)

Symbol error rates with set  $N_f$  and the normal two training symbols passed to MPSync are listed in Table 4. In the series A trials, average SNR at the 0.60 m distance was 6.1 dB.

Due to hardware problems in the series B trials, the average SNR was  $-1.0$  dB, so estimated  $N_f$  was expected to be lower than the actual number present. Fig. 7 illustrates how a weaker path at 6 ms is detected at higher SNR when compared with Fig. 8, where the weak path at 6 ms is usually not detected.

### B. Long distance (12.7 m)

Problems with our hardware limited system performance at the longer 12.7 meter distance during both the A and B test series. In the series A trials, SNR was sufficiently low that poor timing acquisition caused high symbol error rates. This could have been improved with use of longer training symbol sequence, but that software had not been integrated into the modem at the time. A sample MIP for the series A trials at the 12.7 m is included as Fig. 9. Synch errors are visible in the MIP, since channel estimates for entire packets are offset as discrete blocks from the rest.

In the series B trials, the SNR was less than  $-12$  dB, so the receiver could not reliably determine whether a signal was present. Thus no results are listed at the 12.7 m distance for any of the series B trials.

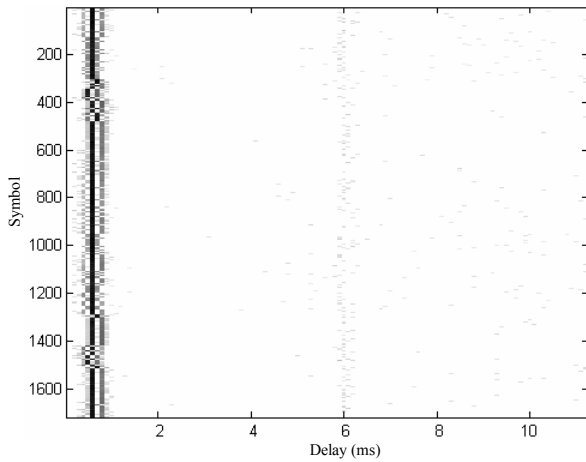


Figure 7. Sample MIP for MSI tank test, fixed  $N_f = 5$ , SNR = 6.1 dB, 0.6 m distance, 2 training symbols.

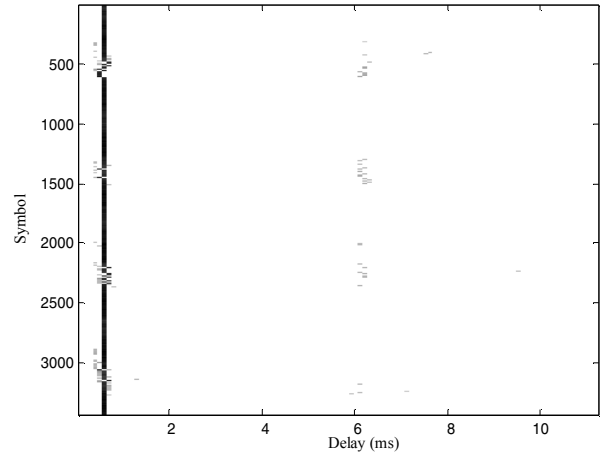


Figure 8. Sample MIP for MSI tank test, estimated  $N_f$  ranging from 1 to 2, SNR =  $-1.0$  dB, 0.6 m distance, 5 training symbols.

Symbol error rates for the 12.7 m distance series A trials are also listed in Table 4, but the Doppler spread calculated from the channel estimates are likely inaccurate due to the high synchronization errors at the 12.7 m distance.

## VII. DOPPLER SPECTRUM PLOTS

Fig. 10 shows Doppler spectrum plots for air and tank tests. In all cases there were unexplained harmonics appearing with magnitude equal to the fundamental, although they are not shown in Fig. 10(b) since the horizontal axis of the plot was magnified to illustrate Doppler spread. This effect might be due to nonlinearity in the system or the periodicity of the packet symbols.

At the 12.7 m distance, the high 0.9 Hz Doppler spread may have been due to incorrect channel estimation due to synchronization errors. Another cause could be the strong currents due to the seawater pumps turning on and off.

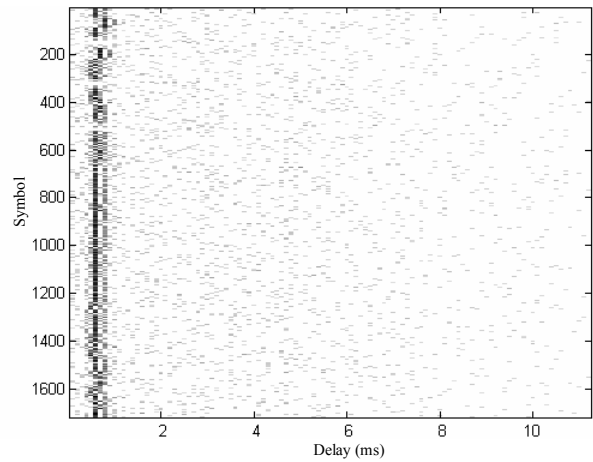


Figure 9. MIP for MSI tank test,  $F_s = 96$  kHz, fixed  $N_f = 10$ , SNR < 6.1 dB, 12.7 m, 2 training symbols

## VIII. CONCLUSION

This paper reported the design and development of an acoustic modem for the application of underwater sensor networks for ecological research. This project represents the direct integration of acoustic data acquisition, communication signal processing, and hardware optimization. This paper also reported the results from a complete sequence of laboratory tests, including wired tests and experiments in air and water chamber for performance evaluation. Full-scale sea tests have also been under preparation. Although this prototype was developed based on the requirements and specifications of typical ecological experiments at various university test sites, with minor modifications it can be generalized and expanded into various underwater sensing applications.

## ACKNOWLEDGMENT

This research program was supported by the Keck Foundation, International Foundation of Telemetry, US Navy, Sonatech, and UC MICRO program.

## REFERENCES

- [1] R. A. Iltis et al, "An Underwater Acoustic Telemetry Modem for Eco-Sensing," in *Proc. MTS/IEEE Oceans*, Washington, D.C., 2005.
- [2] S. Kim and R. A. Iltis, "A Matching Pursuit/GSIC-Based Algorithm for DS-CDMA Sparse Channel Estimation," *IEEE Signal Processing Letters*, vol. 11, January 2004, pp. 12-15.
- [3] S. Mallat and Z. Zhang, "Matching pursuits with time-frequency dictionaries," *IEEE Transactions on Signal Processing*, vol. 41, December 1993, pp. 3397-3415.
- [4] S. F. Cotter and B. D. Rao, "Sparse channel estimation via matching pursuit with application to equalization," *IEEE Transactions on Communications*, vol. 50, March 2002, pp. 374-377.
- [5] D. Doonan et al., "Design and experimentation with a software-defined acoustic telemetry modem," in *Proc. Intl. Telemetry Conf. 2006*, in press.

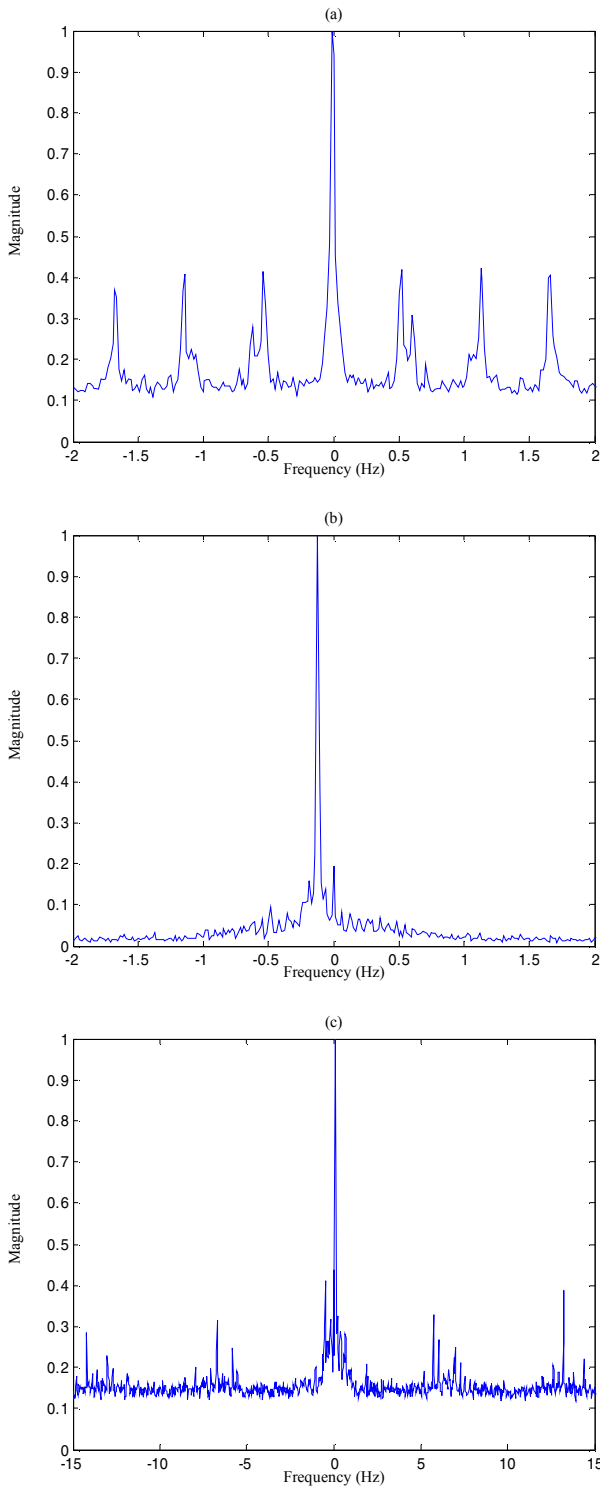


Figure 10. Normalized Doppler spread spectrum plots from channel estimates:  
(a) Hallway air test,  $F_s = 8$  kHz, (b) Trial 2 tank test at 0.60 m,  $F_s = 96$  kHz,  
(c) Trial 1 tank test at 12.7 m,  $F_s = 96$  kHz